Heliospheric Structure: The Bow Wave and the Hydrogen Wall[1]

G.P. Zank(1), J. Heerikhuisen(1), B.E. Wood, (2), N. Pogorelov(1), E. Zirnstein(1), S. Borovikov (1), D.J. McComas(3)

(1)Center for Space and Aeronomic Science (CSPAR)
and Department of Physics
University of Alabama, Huntsville
(2)Naval Research Laboratory
(3) Southwest Research Institute

CSPAR-UAH

Recent IBEX observations [McComas et al. (2012)] indicate that the LISM flow speed is less than previously thought (23.2 km/s rather than 26 km/s).

Reasonable local interstellar medium (LISM) plasma parameters indicate that the LISM flow may be either marginally super-fast magnetosonic or sub-fast magnetosonic.

This raises two challenging questions,
1. *can a LISM model that is barely supersonic or subsonic account for Lyman-alpha observations that rely critically on the additional absorption provided by the hydrogen wall? And*

2. *if the LISM flow is weakly supersonic, does the transition assume the form of a traditional shock or does neutral hydrogen (H) mediate shock dissipation and hence structure through charge exchange?*

Both questions are addressed using three 3D self-consistently coupled MHD plasma - kinetic H models with different LISM magnetic field strengths (2, 3, and 4 G) and plasma and neutral H number densities.

	$|\mathbf{B}|$ (μG)	$\mathbf{B}/|\mathbf{B}|$ (J2000)	n_p (cm^{-3})	T (K)	$|\mathbf{u}|$ (km/s)	n_H (cm^{-3})	M_A	M_f
Model 1	2	$(41, -39)$	0.13	6200	23.2	0.22	1.91	1.64
Model 2	3	$(45, -44)$	0.095	6200	23.2	0.195	1.09	1.03
Model 3	4	$(36, -48)$	0.048	6200	23.2	0.164	0.57	0.56

Table 1: LISM plasma, magnetic field, and neutral H parameters for the three models. Here $|\mathbf{B}|$ denotes the magnitude of the local interstellar magnetic field, $\mathbf{B}/|\mathbf{B}|$ the orientation of the LISM magnetic field, n_p and n_H the plasma and neutral H number density, $|\mathbf{u}|$ the LISM flow speed, M_A the Alfvén Mach number, and M_f the fast magnetosonic Mach number in the distant LISM (taken to be 1000 AU in our simulations).

All the models have a H number density $n_H \sim 0.1$ cm^{-3} at the HTS, and a heliocentric distance to the HTS of about 89 AU in the Voyager 1 and Voyager 2 directions. These parameters are generally accepted values that are consistent globally with almost all observations, whether indirect or direct, e.g., ribbon, HTS location, H deflection, ...

CSPAR-UAH

We use the Huntsville 3D MHD plasma – kinetic neutral H code MSFLUKSS
[Pogorelov, Zank, & Ogino (2004, 2006); Pogorelov, Heerikhuisen, & Zank
(2008); Pogorelov et al. (2011); Heerikhuisen, Florinski, & Zank (2006); Heerikhuisen et al.
(2007)]
*with a kappa distribution (with κ = 1.63 everywhere) for the inner*
heliosheath plasma
[Heerikhuisen et al. (2008), see Livadiotis & McComas (2009)]

We consider a steady-state solar wind model with standard parameters at 1 AU: n_p(1AU) = 7.4 cm^{-3}; T_p(1 AU) = 51,100 K; U_{SW}(1 AU) = 450 km/s and |B| (1 AU) = 37.5 μG.

In all three cases, the HTS is located at approximately the same distance, ~89 AU, along the Voyager 1 and 2 trajectories.
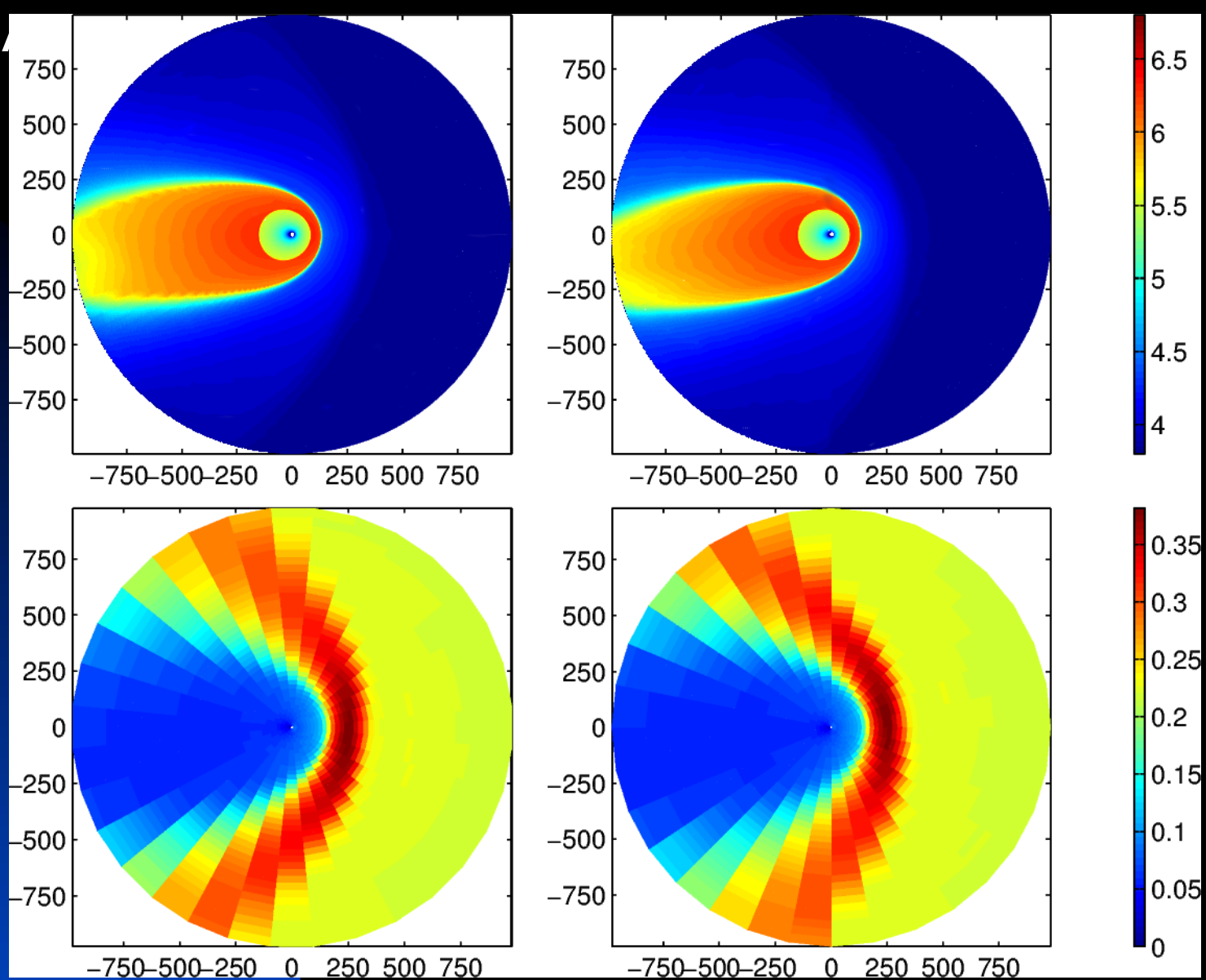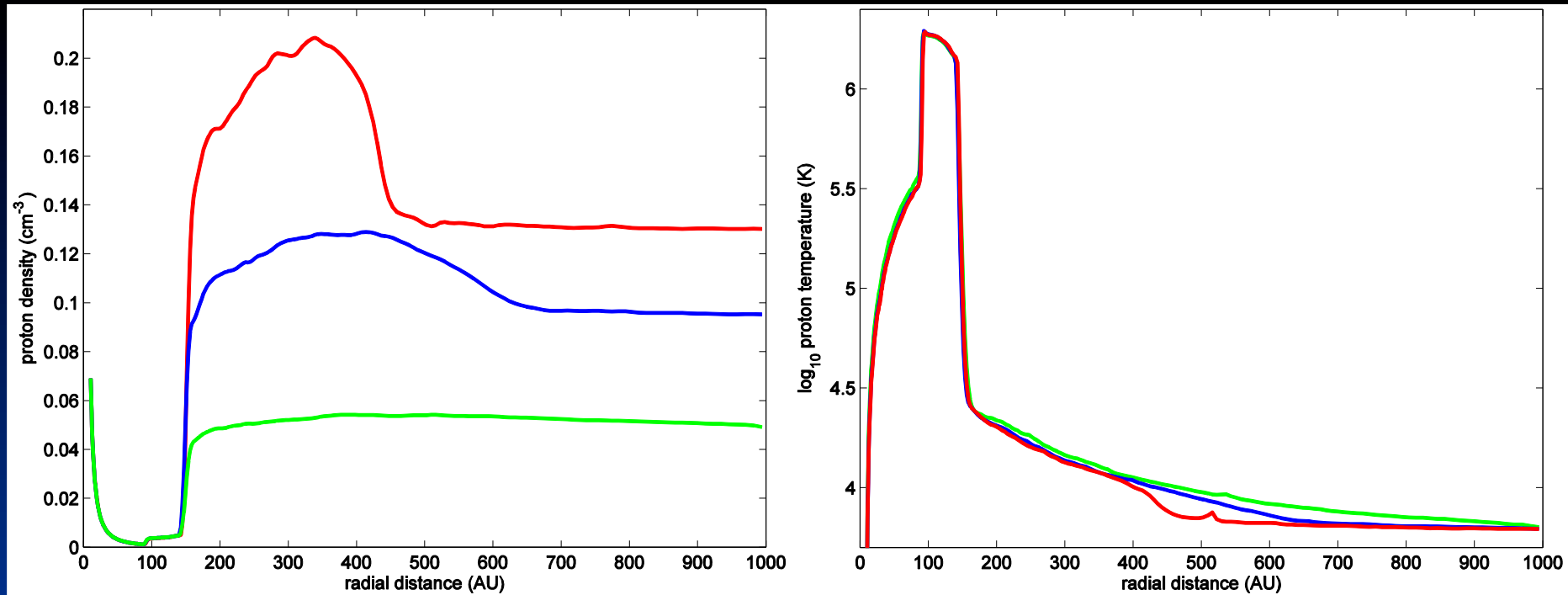
Model 1 (2 mG) plots of the logarithm of the plasma temperature T_p (K) (top row) and neutral H number density n_H (cm−3) (bottom row) plotted in the ecliptic (left column) and polar (right column) planes.
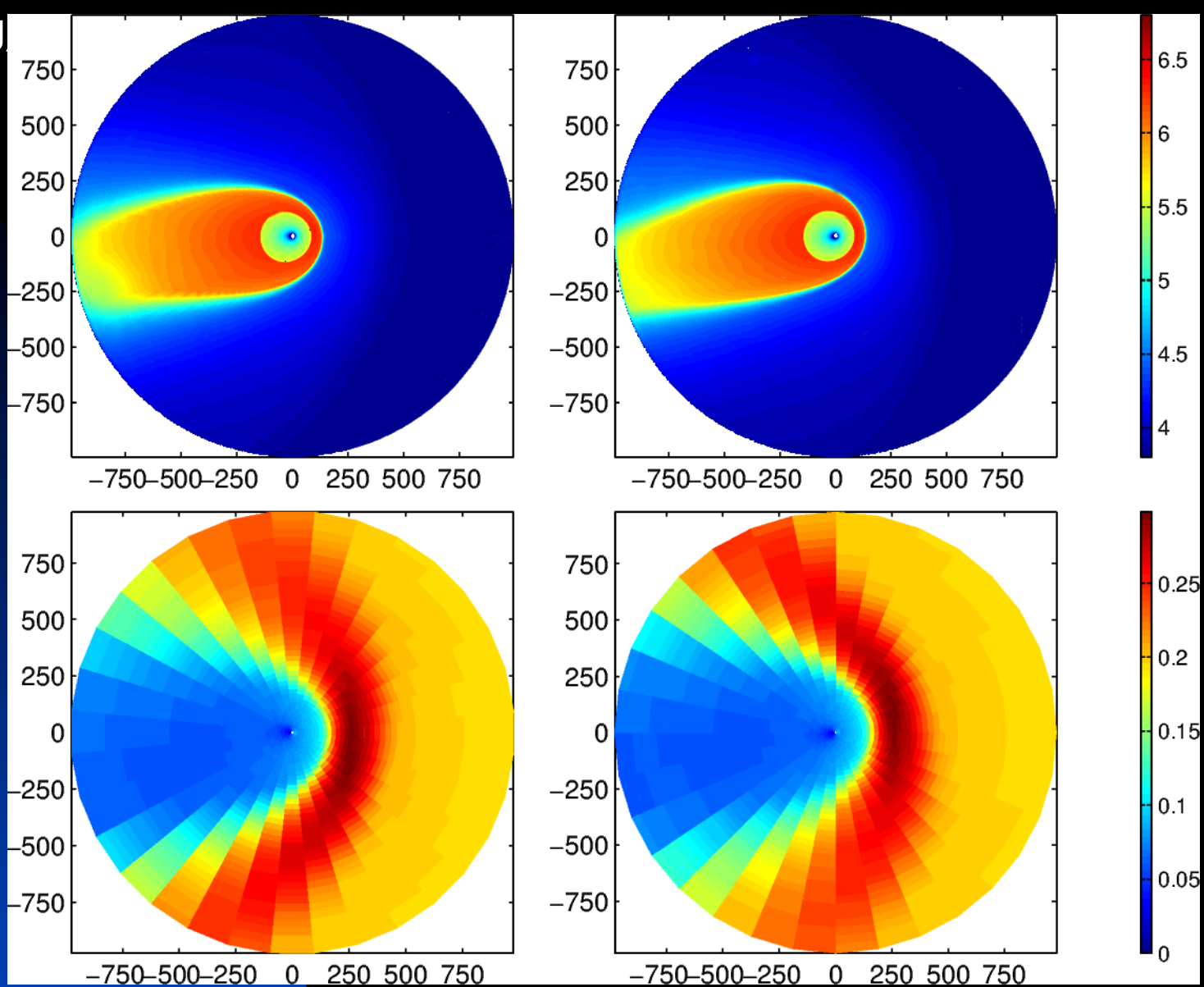
Model 2 (3 mG) plots of the logarithm of the plasma temperature T_p (K) (top row) and neutral H number density n_H (cm−3) (bottom row) plotted in the ecliptic (left column) and polar (right column) planes.
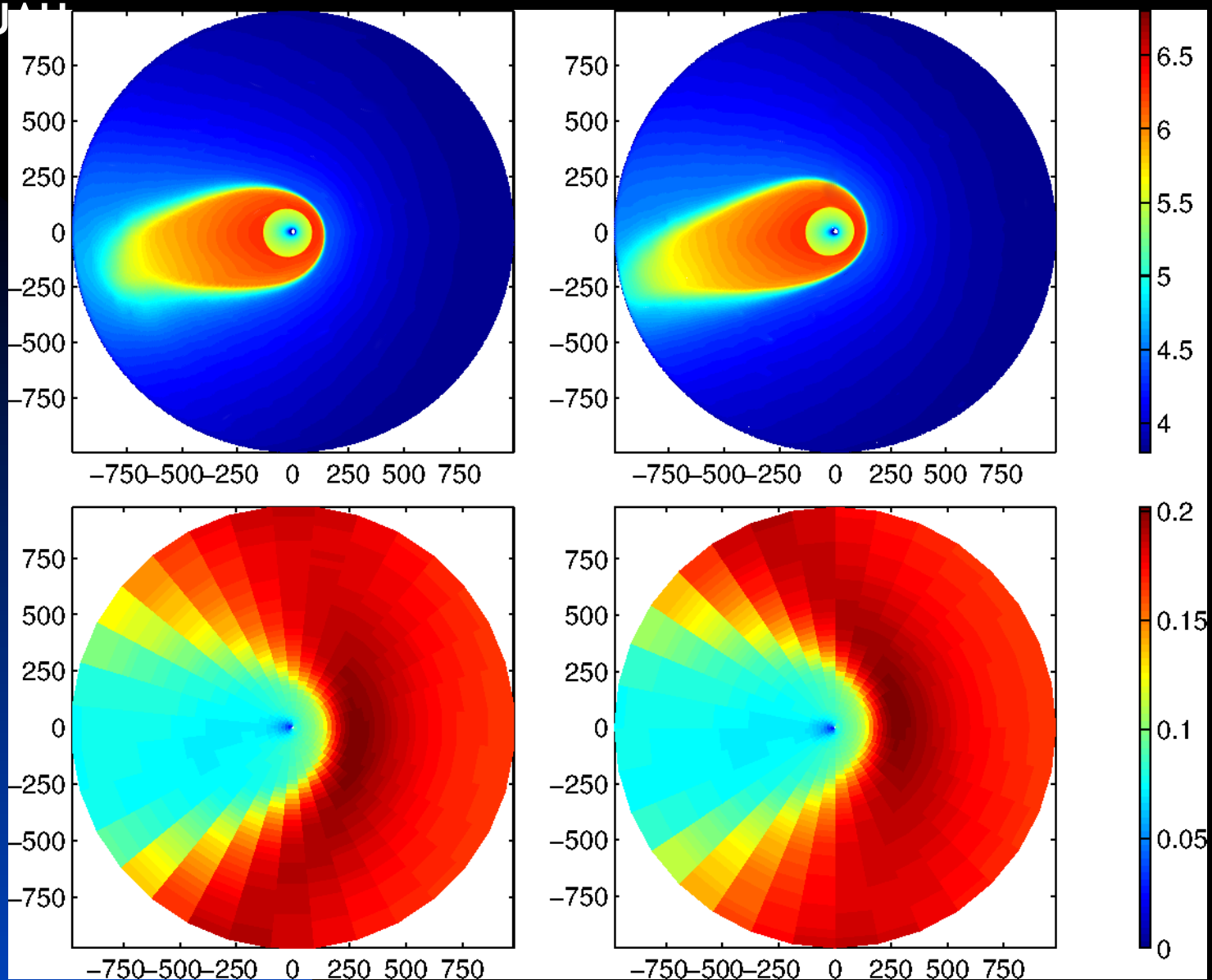
Model 3 (4 mG) plots of the logarithm of the plasma temperature T_p (K) (top row) and neutral H number density n_H (cm^{-3}) (bottom row) plotted in the ecliptic (left column) and polar (right column) planes.

Left: Line plots of the plasma density for Models 1 (red), 2 (blue), and 3 (green) along the a-Cen line of sight. (Right) Corresponding logarithmic plasma temperature line plots for Models 1 - 3 along the a -Cen line of sight.
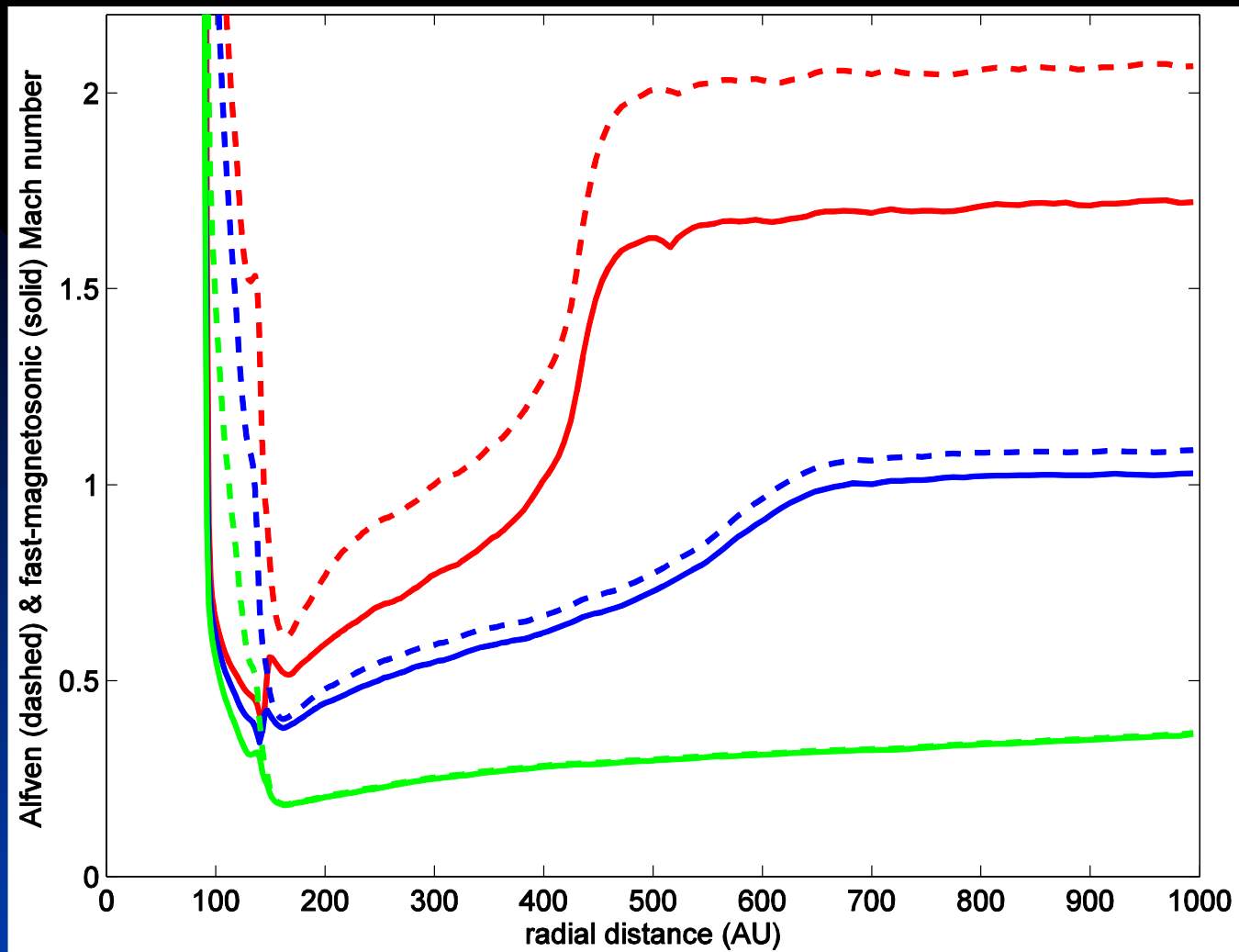
The solid curves show the fast-magnetosonic Mach number M_f for each of the three models (red - 2 mG; blue - 3 mG; green - 4 mG), and the corresponding dashed lines show the Alfven Mach number M_A along the a-Cen sightline. For Model 3, $M_f \sim M_A$ in the LISM until the heliopause.
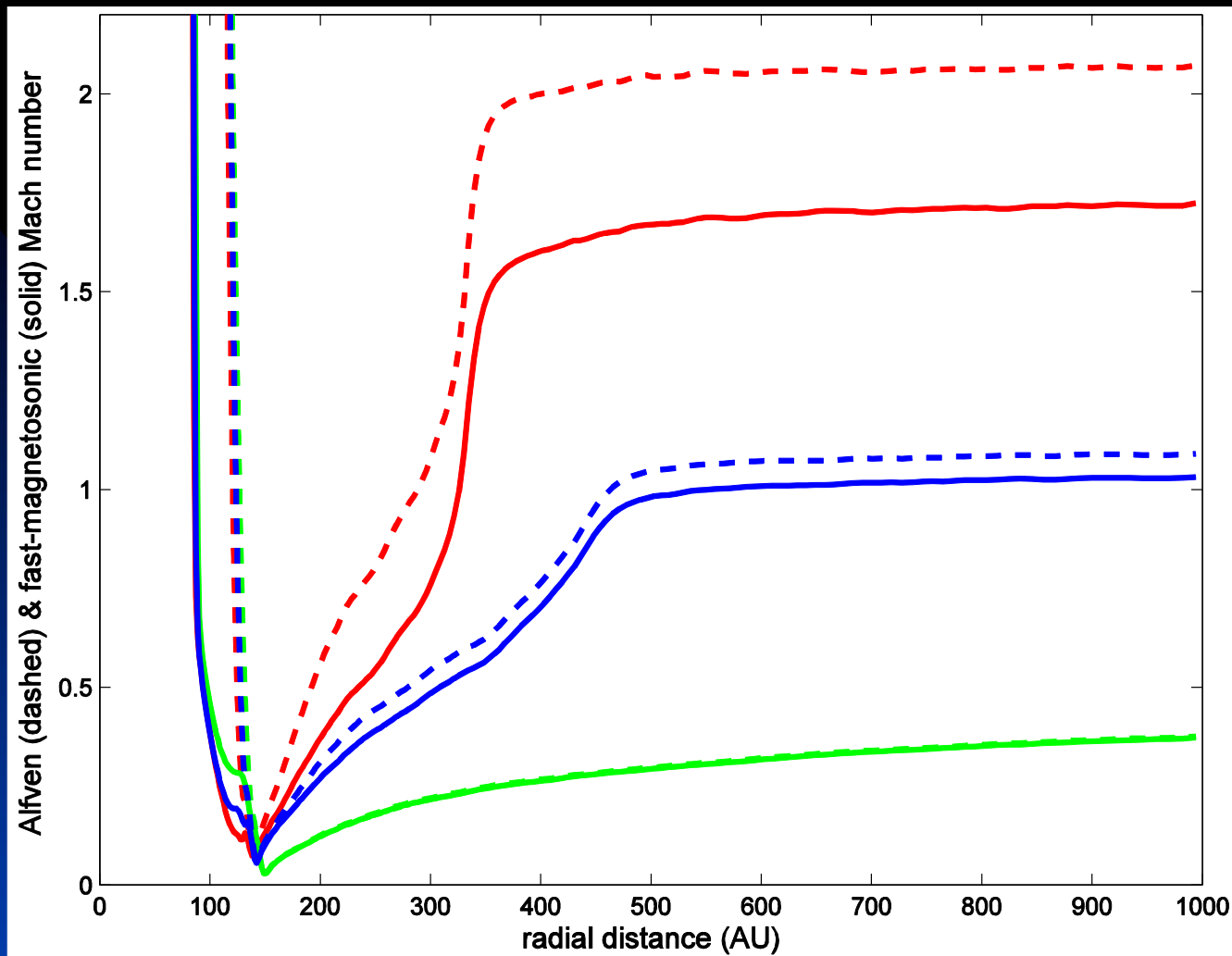
The solid curves show the fast-magnetosonic Mach number M for each of the three models (red - 2 mG; blue - 3 mG; green - 4 mG), and the corresponding dashed lines show the Alfven Mach number M_A along the nose sightline. For Model 3, $M_f \sim M_A$ in the LISM until the heliopause.
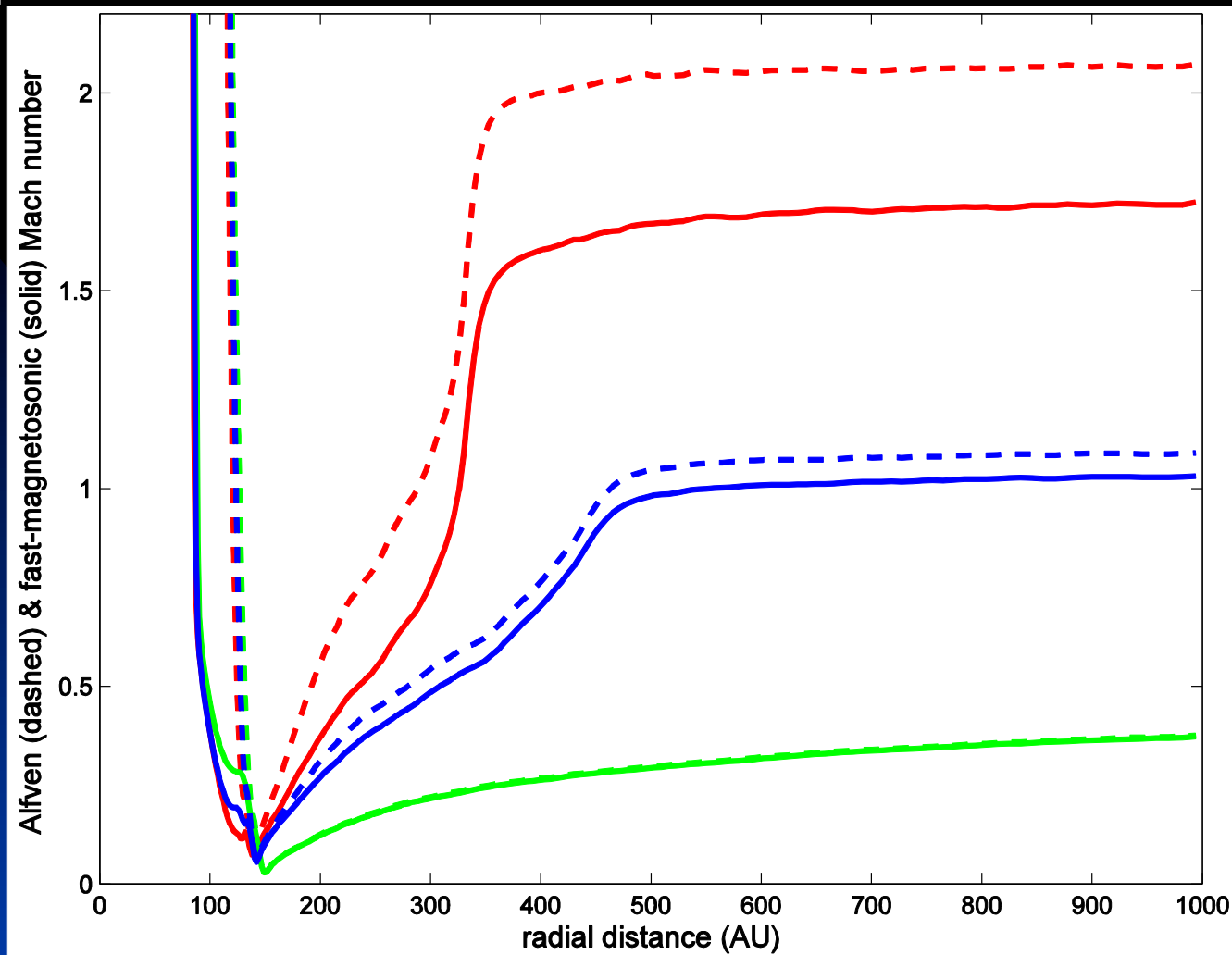
For the 2 mG model 1, the bow shock is located at ~ 360 AU with a width of ~ 40 AU and M_f = 1 at ~ 330 AU. The 3 mG model 2 begins its transition from a super-fast magnetosonic state to one that is sub-fast at ~ 600 AU and has a width of ~ 200 AU, and M_f = 1 at ~ 550 AU.

Structure of the bow wave transition – idealized model in nose direction

$$\mathbf{U} = (U_x, 0, 0), \qquad \mathbf{B} = (0, B_y, B_z).$$

$$\frac{d}{dx}(\rho U_x) = 0 \qquad \Longrightarrow \qquad \rho U_x = \alpha = \text{const.};$$

$$\rho U_x \frac{dU_x}{dx} + \frac{dP}{dx} - \frac{1}{4\pi}\left(B_y \frac{dB_y}{dx} + B_z \frac{dB_z}{dx}\right) = Q_{mx};$$

$$\frac{d}{dx}\left(\frac{1}{2}\rho U_x^3 + \frac{\gamma}{\gamma - 1}U_x P + \frac{1}{4\pi}U_x B^2\right) = Q_e;$$

$$U_x B_y = \text{const.}; \qquad U_x B_z = \text{const.};$$

*The source terms Q_m and Q_e are **non-zero in the ISM** only because of the secondary charge exchange of fast and hot heliospheric neutral H.*

$$\frac{\alpha V_f^2}{\gamma - 1}\left(M_f^2 - 1\right)\frac{1}{U_x}\frac{dU_x}{dx} = Q_e - \frac{\gamma}{\gamma - 1}U_x Q_{mx};$$

$$\frac{1}{\gamma - 1}\frac{M_f^2 - 1}{M_f^2}\frac{dP}{dx} = \frac{U_x^2 - V_A^2}{U_x^3}Q_e - \frac{U_x^2 - V_A^2 - \frac{1}{\gamma-1}C_s^2}{U_x^3}U_x Q_{mx}.$$

*For a **critical point** to exist, both the LHS and RHS must be zero simultaneously. Obviously, the LHS vanishes for $M_f^2 = 1$. For a critical point to exist requires simultaneously*
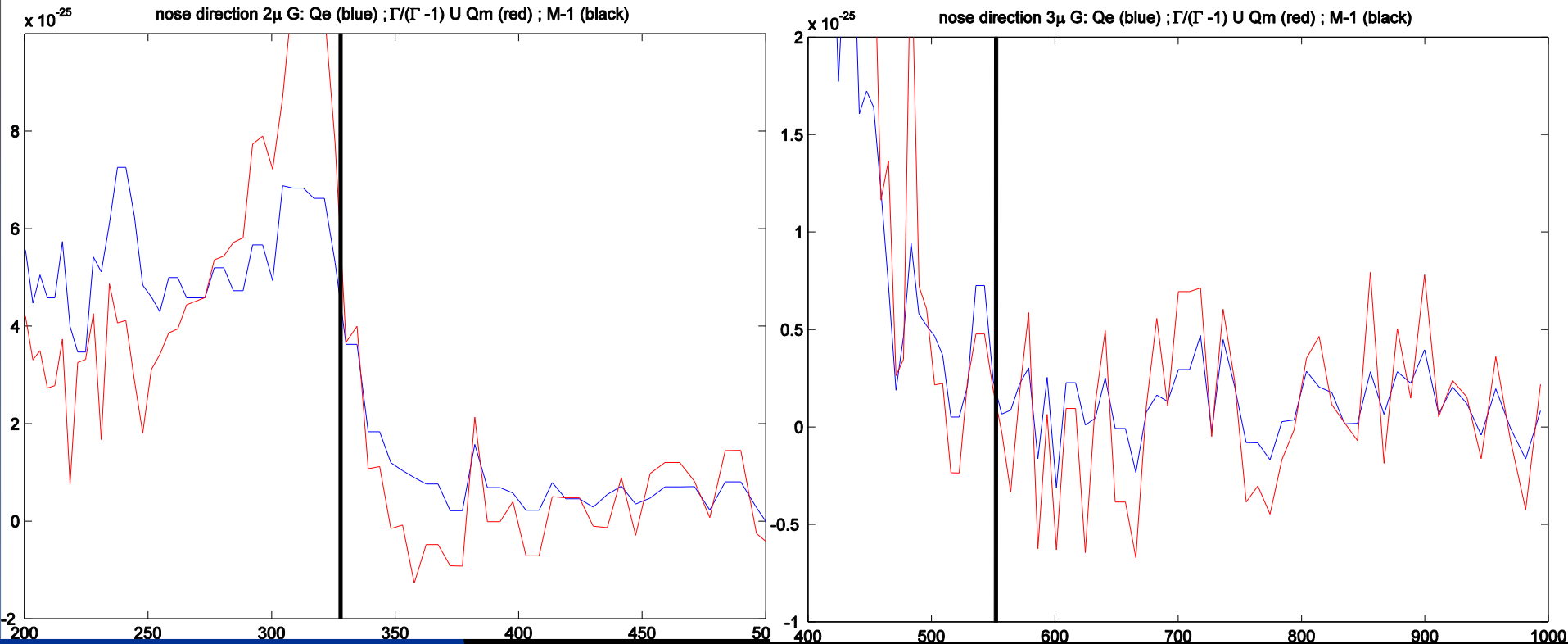
$$Q_e = \frac{\gamma}{\gamma - 1}UQ_m,$$

$$\left(U_x^2 - V_A^2\right)Q_e = \left(U_x^2 - V_A^2 - \frac{1}{\gamma - 1}C_s^2\right)U_x Q_{mx}.$$

Use of the first relation in the second shows this reduces to $M_f^2 = 1.$

*Given the smooth solutions exhibited in the 1D cuts, the critical point would appear to be a **saddle point**, ensuring that the heliospheric - LISM <u>flow transition can possess a</u> smooth decelerating structure that is not a shock.*

Plots of $\gamma / (\gamma - 1) U_x Q_{mx}$ (red curve) and Q_e (blue curve) along the nose direction for (left) the 2 mG Model 1, and (right) the 3 mG Model 2. Also plotted as a vertical line is the location of the $M_f = 1$ line.
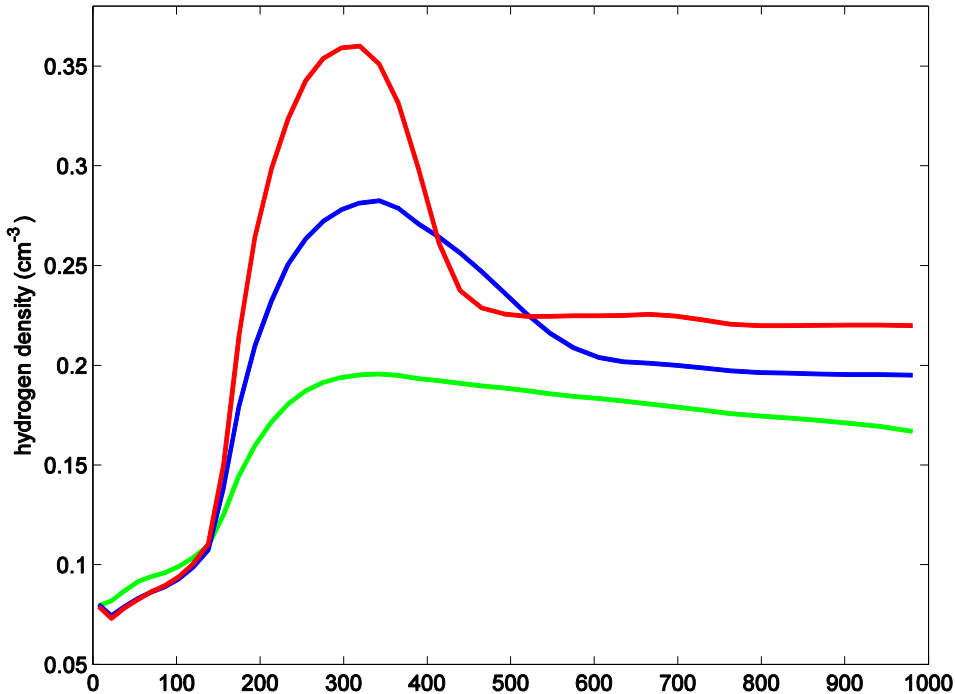
1D plots of the neutral H number density (top left), neutral H temperature (bottom left), and neutral H velocity (bottom right) along the a-Cen sightline for Model 1 (red curve), Model 2 (blue curve), and Model 3 (green curve).

$$\tau(\lambda) = \frac{7.5 \times 10^{-13}}{b_H} N_H e^{-(247\lambda - U_H)^2/b_H^2}$$
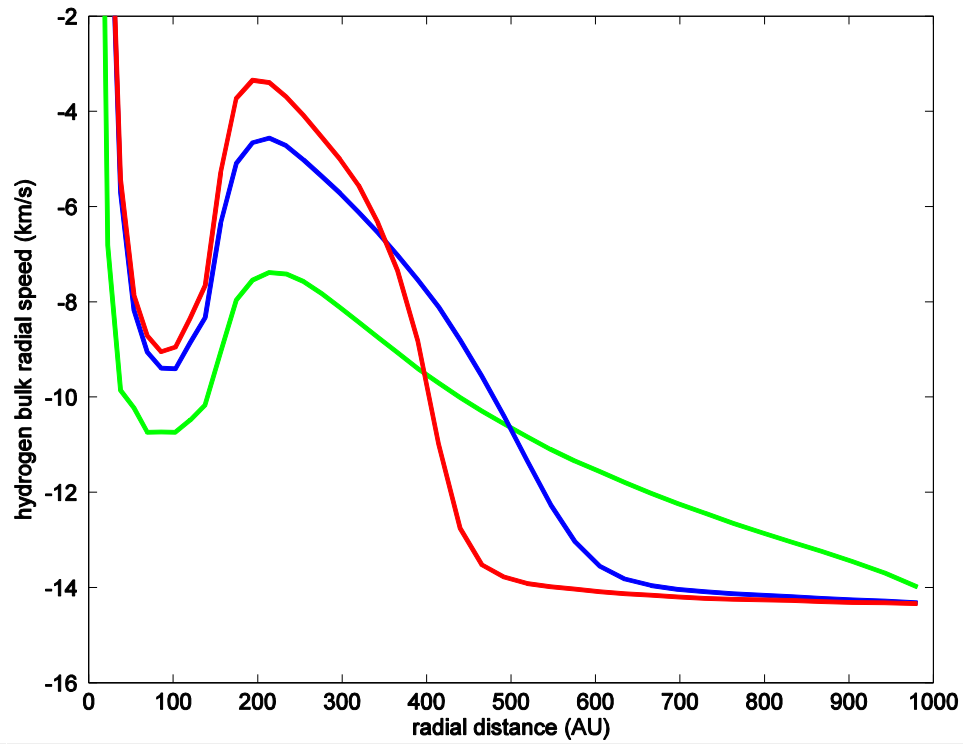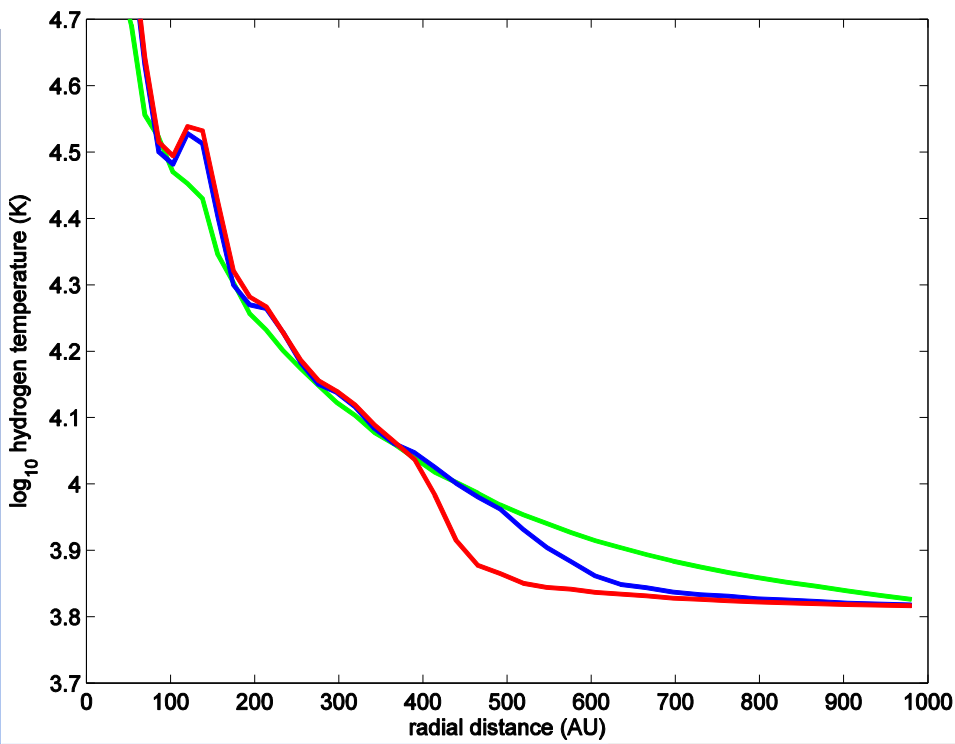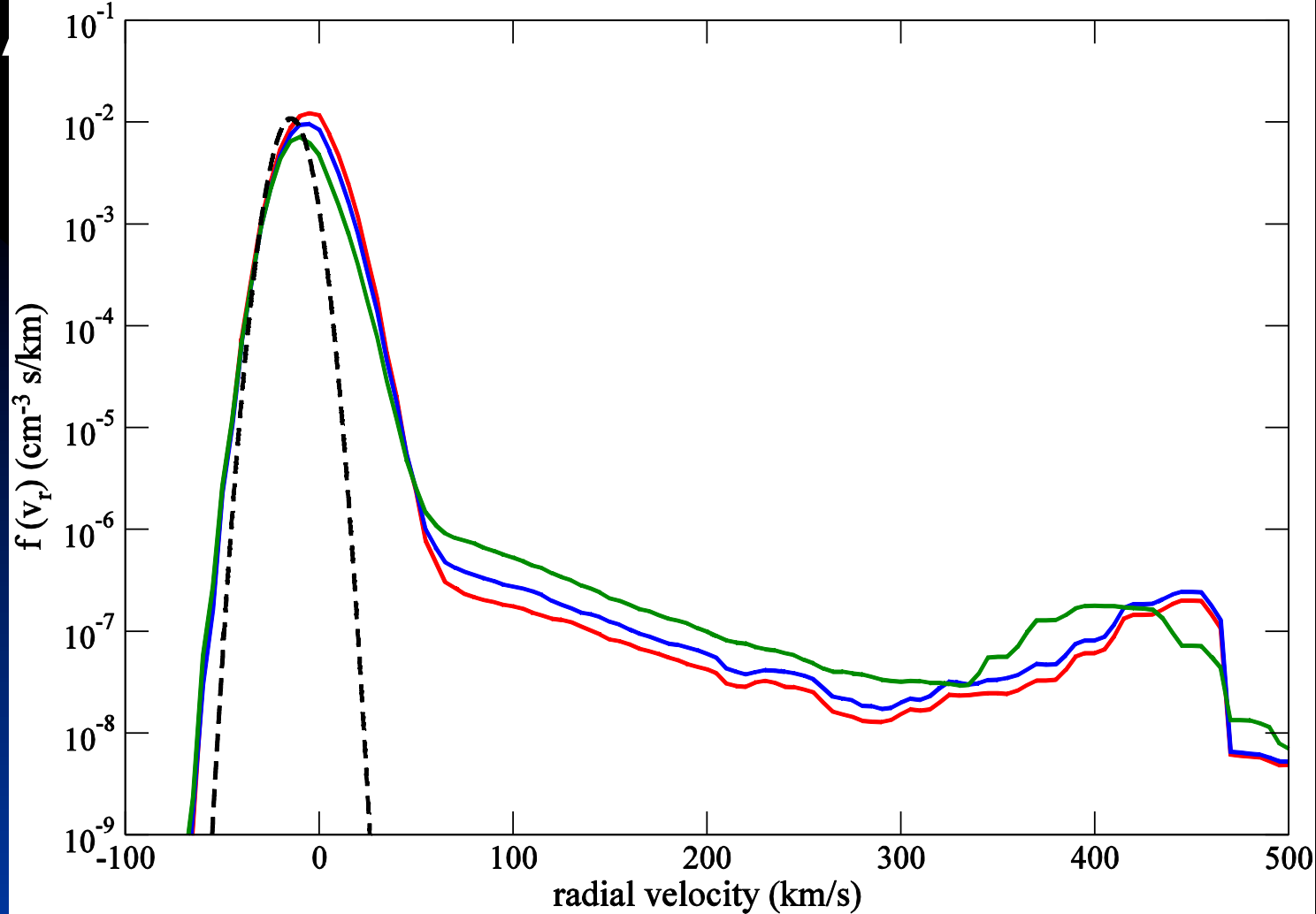
The 1D radial velocity distribution function for neutral H at 300 AU along the -Cen sightline. The red curve shows the Model 1 reduced distribution function, the blue curve that for Model 2, and the green curve is for Model 3. The black dashed line corresponds to the Maxwellian distribution assumed at 1000 AU as the boundary condition distribution for kinetic neutral H model.
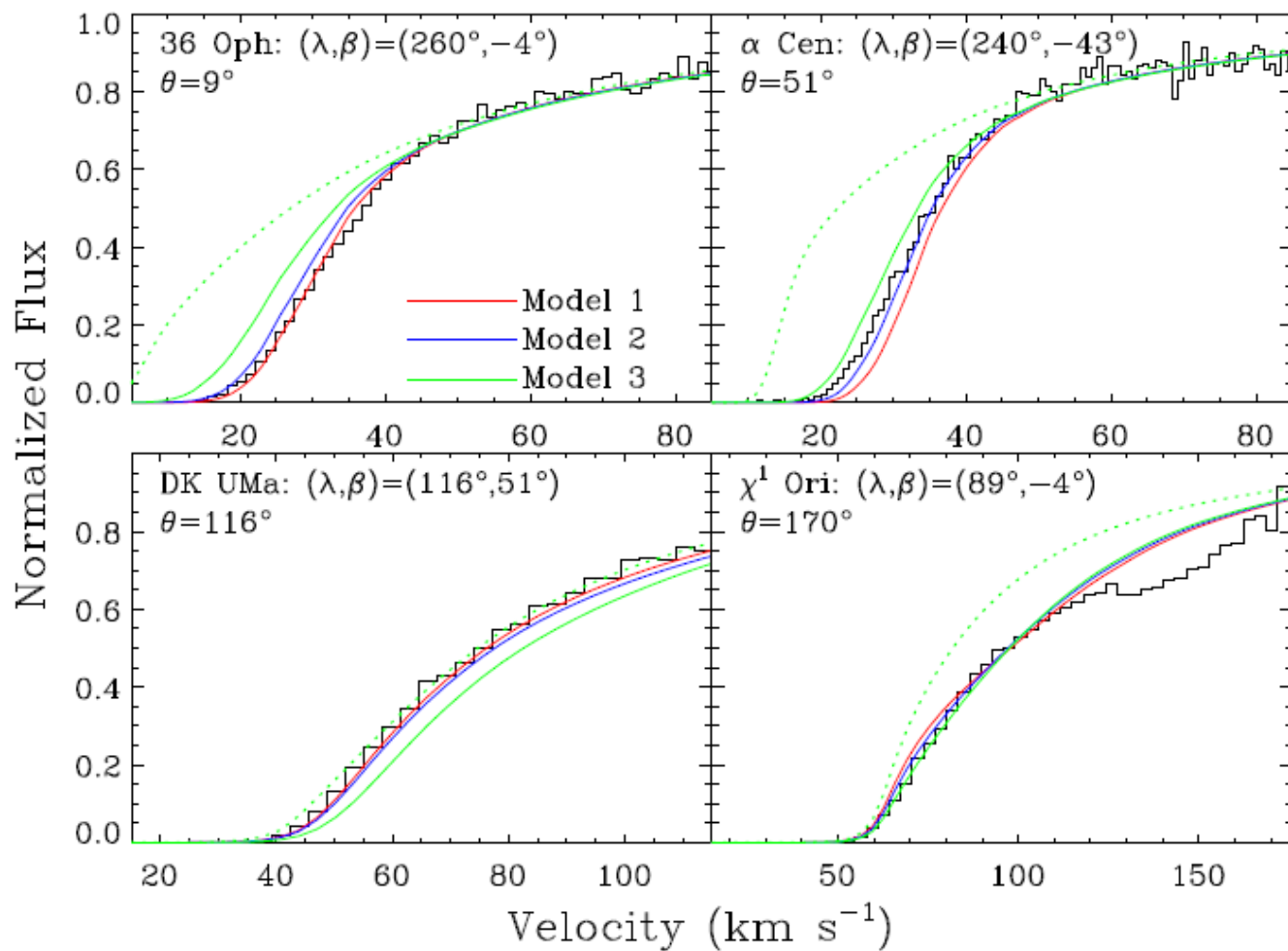
Normalized Lyman-a spectra in four directions, 36 Oph (= 9⁰), Cen (= 51⁰), DK UMa (= 116⁰), and 1 Ori (= 170⁰), showing only the red side of the Lyman-a absorption line since this corresponds to heliospheric absorption. The dotted line shows the expected absorption from the LISM neutral H population alone. The thin black line with steps is the observed absorption along the four sightlines. The red curves correspond to Model 1, the blue curves to Model 2, and the green curves to Model 3.

Summary

1. Is a LISM model that is barely super- or sub-fast magnetosonic consistent with Lyman-a absorption measurements along multiple sightlines, since the interpretation of the Lyman-a observations relies critically on the additional absorption provided by the H-wall?

2. If the LISM flow is weakly supersonic and a shock transition of some kind is necessary, what then is the basic dissipation mechanism, and hence structure, of the shock? Weak collisionless shocks in the solar wind are thought to be laminar [e.g., Formisano (1977)] but in a partially ionized plasma such as the LISM, does charge exchange play a role in shock dissipation process?

CSPAR-UAH

1) We find that a super-fast magnetosonic flow admittes a critical point in the flow when $M_f = 1$ and $Q_e = \gamma (\gamma - 1) UQ_m$ simultaneously.

2) For both Model 1 and Model 2, the LISM flow passes through the CP in transitioning from a supersonic to a subsonic state. Thus, fast and hot neutral H created in the heliosphere mediates the bow shock via charge exchange. Mediation only partial in two-shock case since flow sufficiently supersonic that an additional dissipation mechanism is needed. For Model 2, fast and hot neutral H completely mediates the shock transition, and imposes the charge exchange length scale on the transition that takes the supersonic upstream state to a subsonic state (~ 200 AU thick).

3) Both supersonic LISM two-shock and shock-free Models 1 and 2 produce H-wall of sufficient column depth to account for Lyman-a observations along a-Cen, 36 Oph, DK UMa, and x^1 Ori sightlines. The subsonic Model 3 possesses small H-wall that cannot account for the Lyman-a observations. Observations may marginally favor the 3 mG shock-free Model 2.

We are left with a tantalizing question: Has IBEX discovered a new class of shock wave mediated by interstellar neutral H?
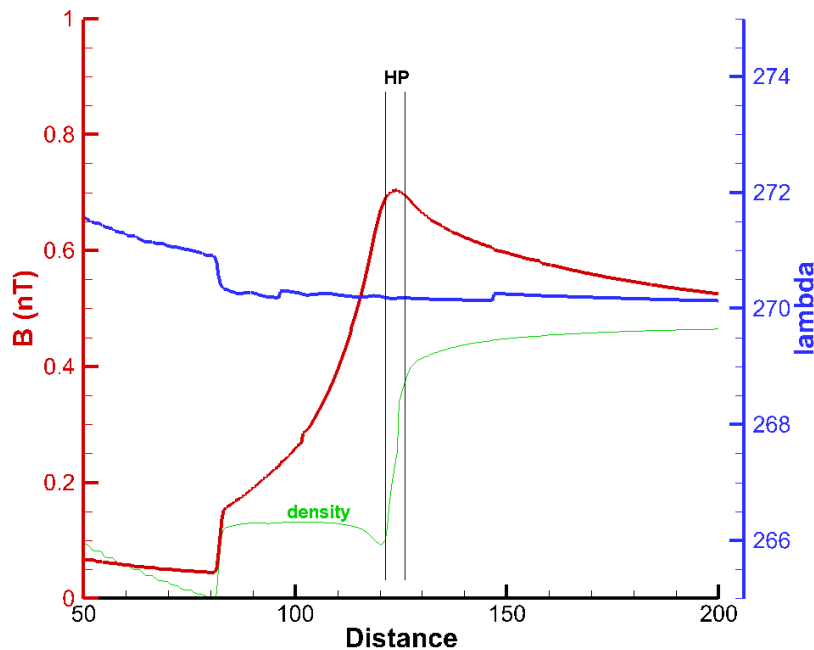
CSPAR-UAH
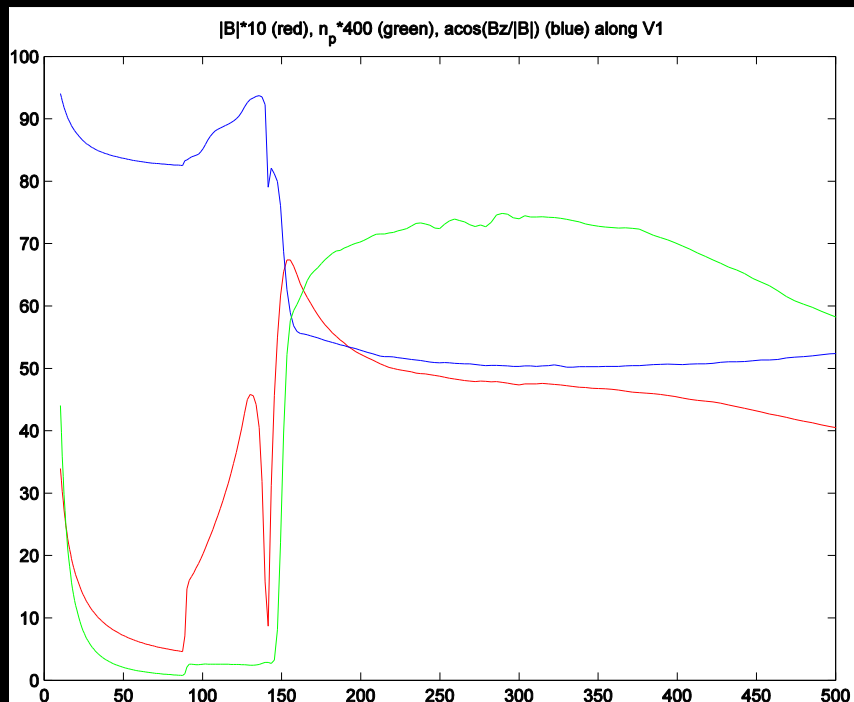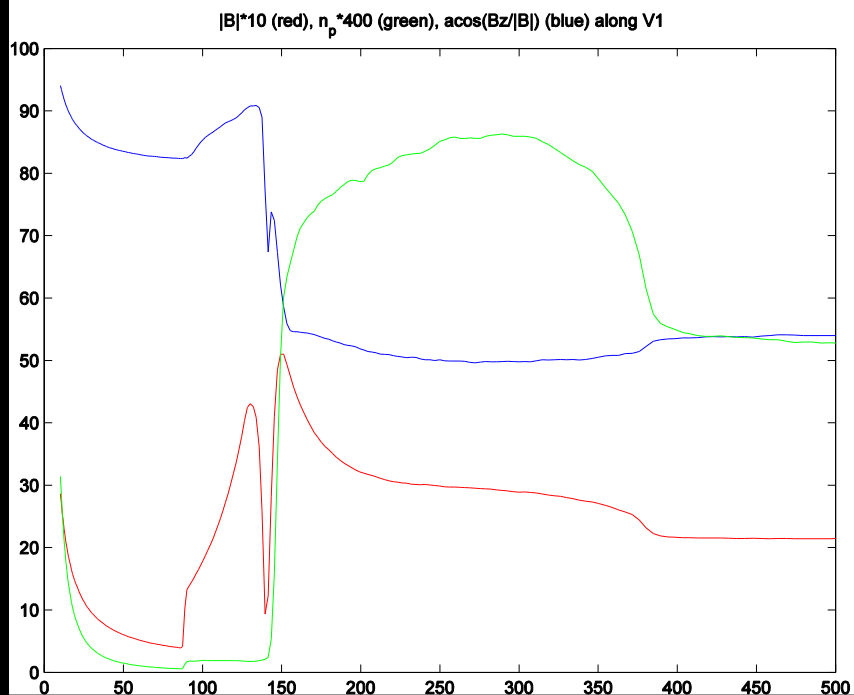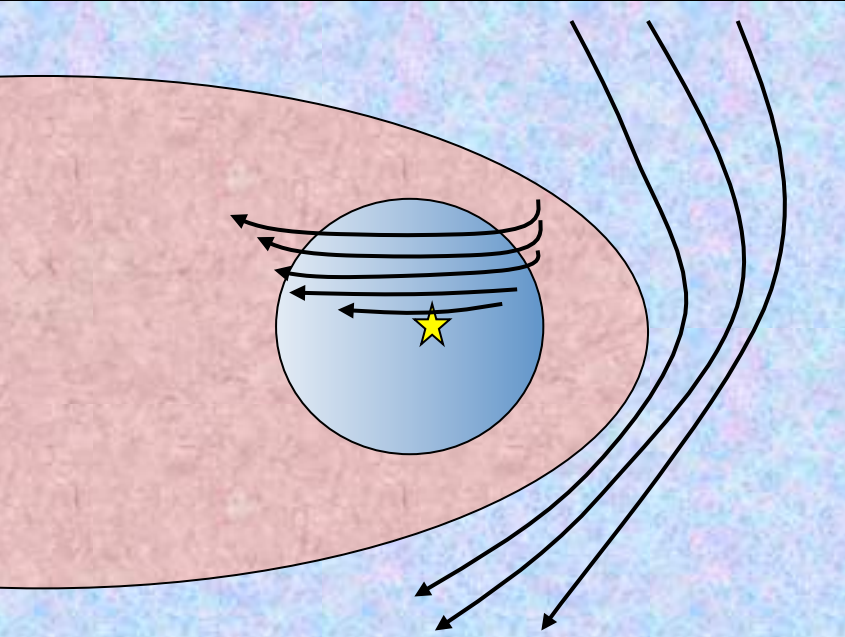
Angle of magnetic field change across HP
~ 50° - 55°
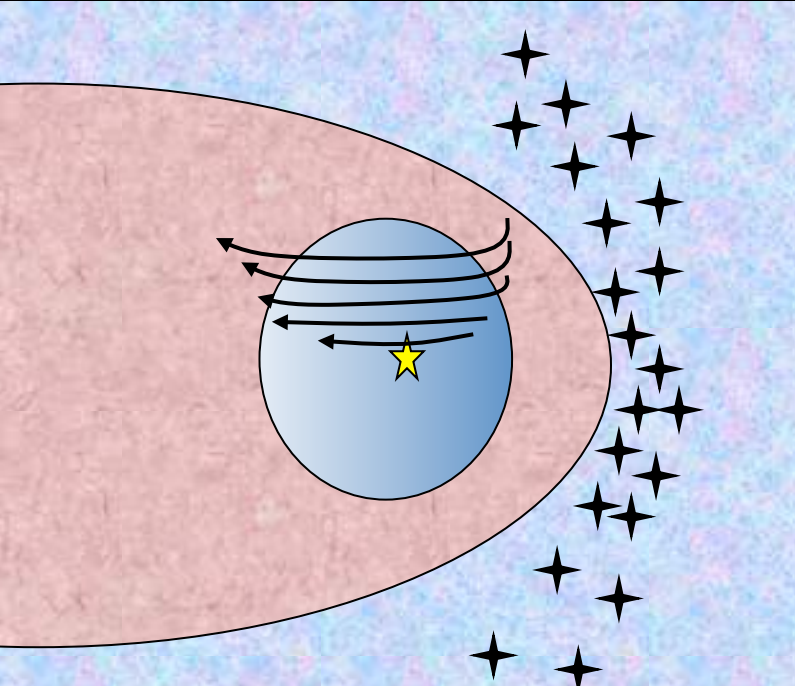
Angle of magnetic field change across HP ~0º

This is only LISM magnetic field configuration that is consistent with V2 magnetic field observations and a HP crossing BUT this would be inconsistent with IBEX BdotR = 0 result for ordering of the ribbon. See Pogorelov et al 2006, ApJ., 2010 (IAC Proc).

Conclusion: no crossing of the HP yet.